Initial leader velocities during intracloud lightning: Possible evidence for a runaway breakdown effect

Sonja A. Behnke, Ronald J. Thomas, Paul R. Krehbiel, and William Rison

Langmuir Laboratory for Atmospheric Research, Geophysical Research Center, New Mexico Institute of Mining and Technology, Socorro, New Mexico, USA

[1]   Using three-dimensional lightning mapping observations, the initial leaders of intracloud flashes have been found to start at a median speed of about 1.6×10^5 m s^{-1} and to decelerate during the first $10-15$ ms of the discharge. The results disagree with the predictions that the speed should increase with time as the developing leader shorts out an increasing potential difference in the storm. The observations can be explained if the flash initiation region is preconditioned in some manner to give a high initial speed and if the preconditioning decays with time and/or decreases with distance to give the observed speed decrease. Such preconditioning could be the result of ionization and excited molecules produced by energetic electron avalanches.

Citation: Behnke, S. A., R. J. Thomas, P. R. Krehbiel, and W. Rison (2005), Initial leader velocities during intracloud lightning: Possible evidence for a runaway breakdown effect, *J. Geophys. Res.*, *110*, D10207, doi:10.1029/2004JD005312.

1.   Introduction

[2]   An important, unresolved question in understanding lightning concerns the manner in which discharges are initiated inside storms [e.g., *Griffiths and Phelps*, 1976; *Solomon et al.*, 2001]. One way of investigating this question is to study the speed with which the initial breakdown propagates inside the cloud. Of particular interest in this regard is study of the breakdown at the beginning of intracloud (IC) lightning discharges.

[3]   Normal-polarity IC flashes are typically initiated between the main negative and upper positive charge regions of a storm and produce a negative leader that propagates upward for $1-2$ km or so before often turning horizontal [e.g., *Shao and Krehbiel*, 1996]. While propagating upward, the conducting leader shorts out an increasingly large potential difference within the storm; consequently the propagation speed of the leader would be expected to increase with time. Also, the speed at the beginning of the leader should provide information on the initiation process itself.

[4]   The leader propagation speeds can be determined by locating the sources of VHF (very high frequency) radiation emitted by the breakdown, using time of arrival or interferometric techniques. From three-dimensional time-of-arrival (TOA) measurements at 300 MHz, *Proctor* [1981] observed initial speeds between 0.9 and 2.1×10^5 m s^{-1}. From two-dimensional interferometric measurements at 274 MHz, *Shao and Krehbiel* [1996] obtained speeds of 1 to 3×10^5 m s^{-1}. From electric field change measurements of the charge transfer during the initial stages of IC flashes, *Liu and Krehbiel* [1985] inferred initial propagation speeds of 1.5 to 3×10^5 m s^{-1}. The different types of observations give consistent results, and the measured velocities also agree with the speeds of downward directed leaders at the beginning of negative cloud-to-ground discharges [e.g., *Schonland*, 1956].

[5]   In this paper we report results in which data from the New Mexico Tech Lightning Mapping Array (LMA) are used to estimate the three-dimensional propagation velocity as a function of time during the initial negative leader of IC discharges. The measured speeds are compared with those expected from a simple model and indicate that preconditioning appears to be present at the beginning of the discharge.

2.   Observations and Results

[6]   We have investigated the propagation velocities of intracloud leaders in three storms. Two of the storms occurred over Langmuir Laboratory in central New Mexico on 2 August 1999 and the third was a small storm on 11 July 2000 during the Severe Thunderstorm Electrification and Precipitation Study (STEPS) in northwestern Kansas and eastern Colorado. In each case the lightning sources were located by a 12- or 13-station mapping array [e.g., *Rison et al.*, 1999; *Krehbiel et al.*, 2000; *Coleman et al.*, 2003; *Lang et al.*, 2004]. The LMA is a time-of-arrival system that operates at $60-66$ MHz and has been described in detail by *Thomas et al.* [2004]. In each case the storm was situated over the central part of the mapping network where the location accuracy is optimal.

2.1.   Flash Examples

[7]   Figure 1 shows observations of an IC flash that occurred in a small storm over Langmuir Laboratory at 2144:57 UT on 2 August 1999. Figures 1e and 1f show the radiation sources in plan and vertical projections. Figures 1b−1d show the temporal development of the
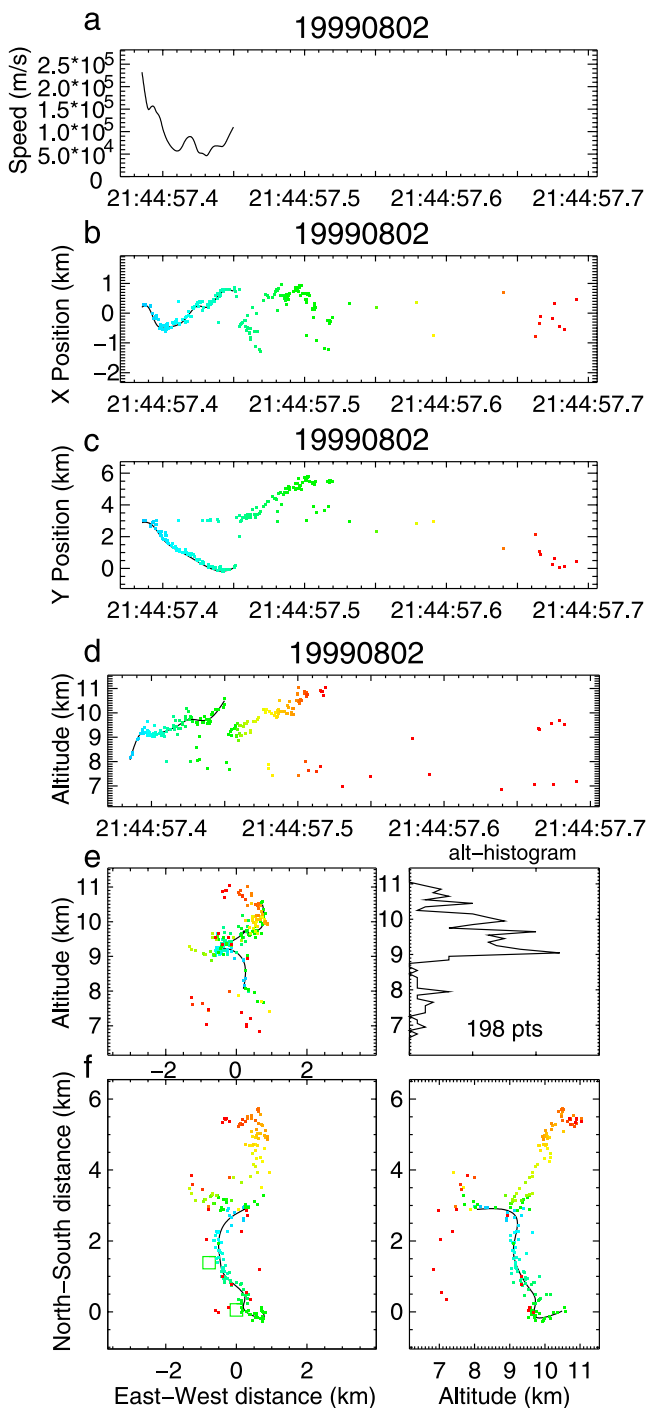
Figure 1. Intracloud flash at 2144:57 UT on 2 August 1999 over Langmuir Laboratory in central New Mexico, illustrating how the initial leader was fitted to determine its three-dimensional propagation speed versus time. (a) Propagation speed versus time; (b−d) x, y, and z (altitude) source locations versus time and cubic spline fits for the initial leader (black curve); and (e and f) plan and vertical projections of the flash and a histogram of the source heights.

source locations in x, y, and z and the measured propagation speed of the initial breakdown. The propagation speed was determined by fitting a smooth curve to the upward initial leader, shown by the black lines.

[8] The Figure 1 flash was a classic bilevel discharge between inferred negative charge at 7−8 km altitude and positive charge at 9−11 km altitude (all altitudes are GPS values and are within about 10 m of mean sea level). The initial source was detected at 8.2 km altitude and the ensuing leader developed upward for 8−9 ms, then turned horizontally southward at the upper level. The leader lasted about 65 ms and traveled about 1 km upward during its initial phase and 3−4 km southward in the upper level. A second leader extended the discharge horizontally northward in the upper level. As is typical of IC flashes observed at VHF, a relatively small number of sources were located in association with positive-polarity breakdown in the lower level.

[9] Figure 2 shows how the source locations were fitted to determine the leader velocity. Smooth curves were independently fit to the x, y, and z source locations versus time and differentiated to give the Cartesian components of the propagation velocity. The fitting was done by means of a cubic spline interpolation through the times of manually selected anchor points, or "nodes." The nodes are indicated by the red triangles in Figure 2, and their times were independently selected for each Cartesian direction. The fitting program varied the spatial position of each node iteratively until the curve best matched the data. The best fit minimized the squared error between the spline and the individual data points, and is indicated by the dashed blue line in Figure 2. In determining the best fit, each source was weighted according to its RMS location uncertainty, indicated by the error bars associated with each point.

[10] In the x and y directions the uncertainties in the source locations were small compared to the scatter of the sources about the best fit. This is reflected quantitatively in the goodness of fit (reduced chi-square) values of the fits, which were $\chi_\nu^2 = 50.7$ and 23.5 respectively in x and y, versus $\chi_\nu^2 = 1-2$ if the data were fitted within the location uncertainties. The same is true of the scatter in z ($\chi_\nu^2 = 16.6$), except that some sources had relatively large (500 m RMS) height uncertainties. The latter resulted from stations beneath or close to the storm happening not to participate in the solutions for the sources in question [Thomas et al., 2004]. The scatter indicates that the leader did not follow a single path, but had side branches that were incompletely mapped by the observations. The fitted curve follows the general progression of the leader reasonably well, however.

[11] We note that the fit and the resultant speed values are sensitive to the time placement of the nodes. Too many nodes cause the fitted curve to have excessive turns or "wiggles," while too few nodes give a fit that does not follow the overall progression. We manually adjust the number of nodes and their times, independently for each direction, to give a reasonable fit, but sometimes there are extra wiggles that adversely affect the velocity values. To avoid overinterpreting small wiggles, we averaged the speed values over successive 5 ms time intervals during the first 15 ms of the leader. The slope of the solid colored lines in Figure 2 indicates the average speed for the intervals 0−5 ms, 5−10 ms, and 10−15 ms. We use the average values
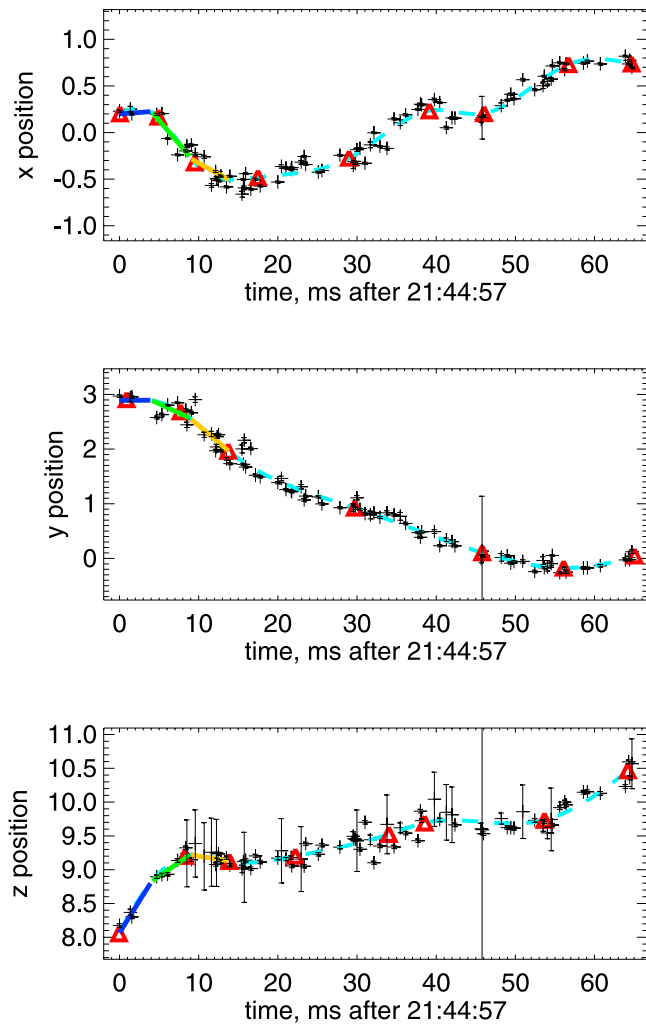
Figure 2. Cubic spline interpolations for the initial leader of Figure 1. The individual source locations (pluses) are shown in km units versus time, with vertical error bars indicating the RMS uncertainty of each location. The red triangles are the anchor points for the interpolated fit (dashed blue line). The slopes of the solid colored lines correspond to the average speed for the time intervals 0−5, 5−10, and 10−15 ms.

later to characterize the leader speeds versus time for a number of IC flashes.

[12] The unaveraged velocity versus time for the flash at 2144:57 is shown in Figure 1a. The leader began with a speed of 2.3×10^5 m s^{-1} and quickly decelerated within about 10 ms to almost half the initial speed. The deceleration interval corresponded to the time the leader was developing upward. Subsequently, during its horizontal development, the leader speed was between 0.5 and 1.0 × 10^5 m s^{-1}, with the fluctuations being associated mostly with back-and-forth motion in the *x* direction.

[13] Figure 3 shows observations of another IC flash that occurred about 13 min later in the same storm as the flash of Figure 1. In the interim the storm moved 3−4 km eastward from its initial location over the laboratory area and grew in vertical extent. The flash began with upward negative

breakdown again starting at 8.2 km altitude, as in the first flash, but progressed about 2 km upward before gradually turning horizontal. The lightning sources indicate that the discharge occurred between inferred positive charge between 10 and 12 km altitude and negative charge between 6 and 8 km altitude.
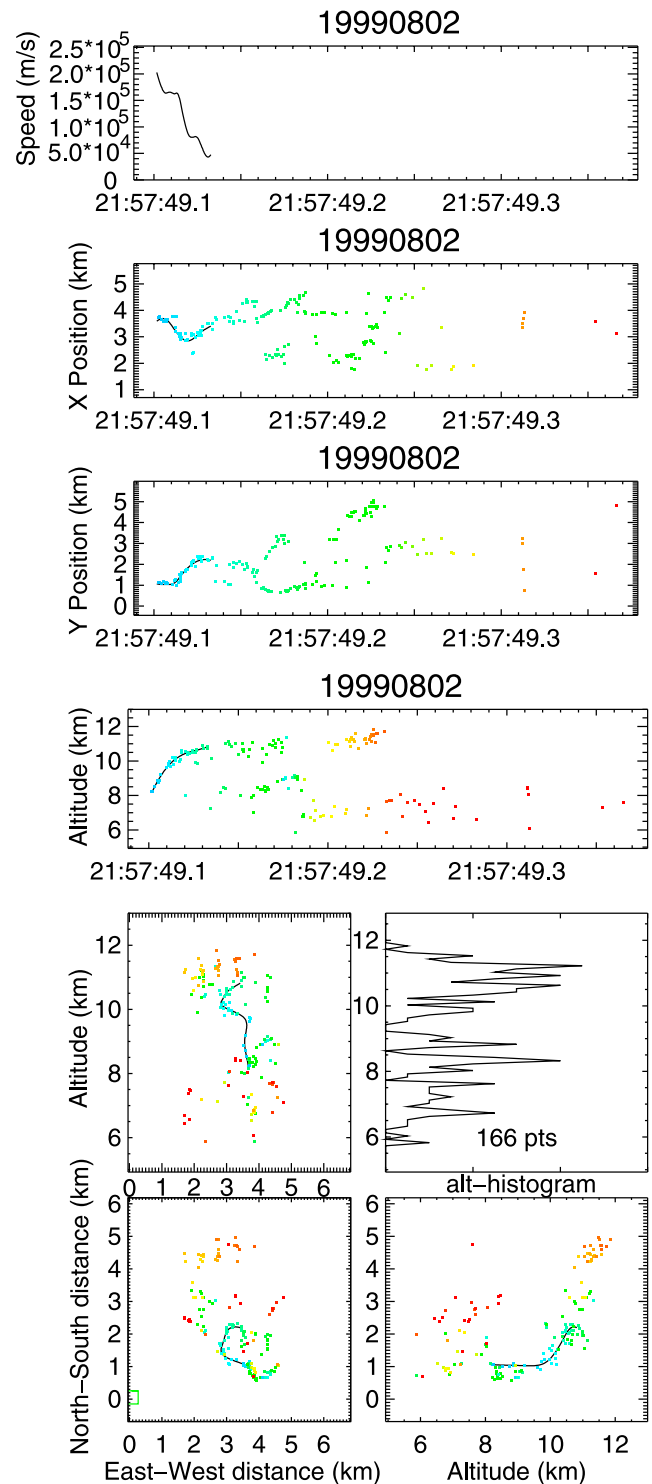
Figure 3. Same as Figure 1, except for an intracloud flash at 2157:49 UT on 2 August 1999.
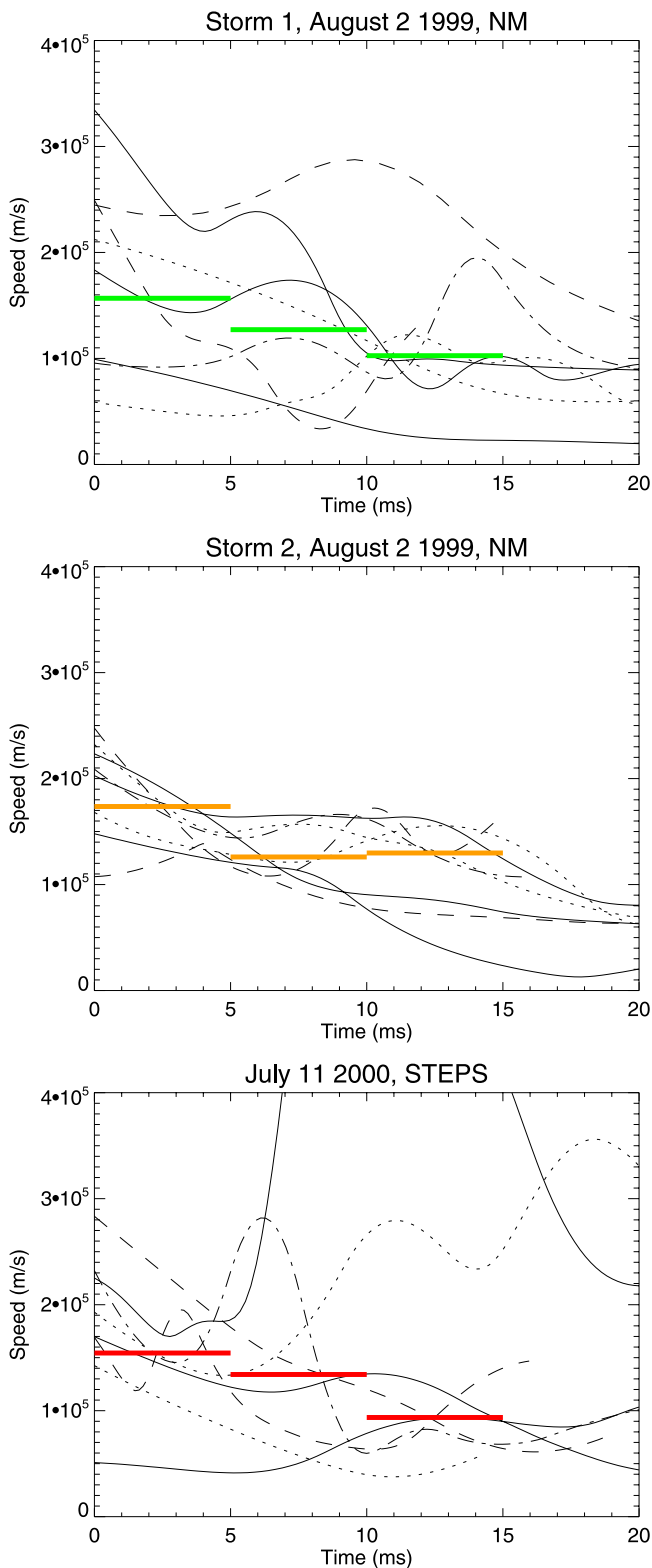
Figure 4. Measured propagation speeds of the initial leaders of 24 intracloud flashes in three storms: two storms in central New Mexico and one in northwestern Kansas during STEPS. The speed of each leader was averaged over the time intervals 0−5, 5−10, and 10−15 ms, and the horizontal colored lines correspond to the median averaged speed in each time interval.

[14] The initial leader was fit with a cubic spline for the first 33 ms of its duration, during which time the discharge progressed from 8 km up to about 11 km altitude. The leader started at a speed of 2.0×10^5 m s^{-1} and steadily decelerated to 0.8×10^5 m s^{-1} after 22 ms. By this time the leader had reached a height of 10.5 km; it subsequently developed eastward and decelerated slightly, to 0.5×10^5 m s^{-1}.

2.2. Overall Results

[15] A total of 24 cloud flashes were analyzed in detail to determine the propagation speed of the initial leaders. These were flashes whose initial leader was well defined and which developed vertically for 1 km or more. About 10% of the cloud flashes met this criteria in each of the storms, but similar results were obtained for almost all flashes that could be analyzed in the three storms and in other storms. Many cloud flashes had an insufficient number of initial sources to accurately determine the speed versus time or had a complex initial structure. The latter included flashes whose initial activity was branched (usually because the flashes were initiated at higher altitude, near the base of the upper positive charge region rather than just above the negative charge region) or, in some instances, which began with a short period of horizontal development prior to turning vertically upward.

[16] Figure 4 shows the propagation speeds of the 24 flashes (8 flashes in each storm). Only the first 20 ms of each flash is plotted, although the fit often extended continuously for 50 ms or more. With the exception of two flashes from the STEPS storm, the speeds generally decreased with time, from initial values typically between 1 and 3×10^5 m s^{-1} to final values on the order of or less than 1×10^5 m s^{-1}. The final leader speeds fluctuated around an approximate equilibrium value, both on the timescale shown in Figure 4 and over the complete duration of the initial activity (e.g., Figures 1 and 3).

[17] As discussed in connection with Figure 2, the speed values were averaged over three consecutive 5-ms time intervals at the beginning of each flash. The horizontal colored lines in each panel indicate the median value of the individual averaged speeds of the flashes analyzed for that storm. The median was considered to be more representative of the typical behavior than the average because of the large apparent fluctuations in several flashes from the STEPS storm.

[18] In the three storms, the median averaged speed during the first 5 ms was consistently between 1.5 and 1.7×10^5 m s^{-1}. The speed decreased to about 1.0×10^5 m s^{-1} by 10 to 15 ms into the flash. The decrease reflected a clear tendency of the individual leaders to decelerate initially with time. The initial speeds agree with the values obtained by previous investigators, as described in the introduction, and expand upon the earlier results by showing how the speed changes with time. As discussed in section 3, the observed deceleration is inconsistent with the expected behavior in an increasing ambient potential difference.

3. Expected Breakdown Speeds: A Simple Model

[19] In this section we simulate the behavior of the initial leader of an intracloud discharge using a simple model to
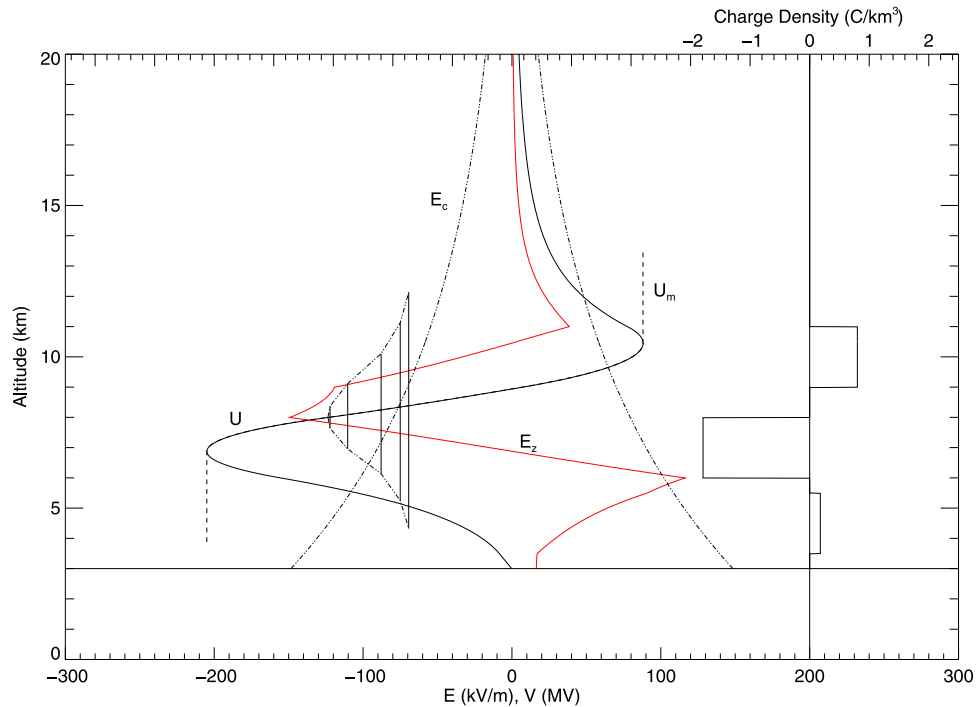
Figure 5. Electric field (red) and potential profiles (black) representative of those in a small New Mexico storm, computed from a simple cylindrical disk charge model (right; Table 1). The charge locations and extents were determined from the lightning mapping observations for the second storm on 2 August 1999, and the charge magnitudes were adjusted to favor the initiation of intracloud flashes, using the critical field for runaway breakdown (dashed line) as a reference for lightning initiation. The vertical lines indicate the simulated development of a bidirectional leader at 5 ms time intervals, for an assumed initial length $L = 100$ m (see text).

estimate the initial propagation speed and how the speed would vary with time.

[20] Figure 5 shows computed profiles of the vertical electric field E_z and the electric potential U that are representative of those observed in small storms. The profiles were obtained using a cylindrical disk model for the storm charges and calculating E_z and U along the z axis through the disks. Three charge regions are used to simulate the tripole structure of small storms and to ascertain the basic conditions in which IC flashes develop. The particular charge parameters used to determine the profiles were inferred from the lightning observations in the second storm on 2 August 1999, and are listed in Table 1 and indicated on the right-hand side of Figure 5. The basic assumption is that the lightning sources and channels reflect the location of net charge in the storm, as shown by *Coleman et al.* [2003]. The 1999 storms occurred over the Magdalena Mountains in the vicinity of Langmuir Laboratory, where ground level is at about 3 km altitude. This is assumed to be the altitude of a ground plane for calculating the second-order effects of image charges, as indicated by the horizontal line in Figure 5. A somewhat similar axisymmetric model was used by *Mazur and Ruhnke* [1998] to study the development of cloud-to-ground and intracloud leaders assuming a constant propagation speed.

[21] To investigate the development of intracloud leaders, the charge amounts were adjusted so that the maximum E_z values exceeded the critical field E_c necessary

for runaway breakdown [*Gurevich and Zybin*, 2001; *Solomon et al.*, 2001]. The runaway threshold was exceeded over an approximate 2 km vertical depth above the main negative charge region. Because the 2 August storm produced few ground discharges, the lower positive charge was chosen such that E_z did not exceed E_c over a significant vertical distance. The critical field is proportional to the air density and is indicated by the dotted lines in Figure 5. That in-cloud electric fields are comparable to the critical field has been shown by *Marshall et al.* [1995].

[22] Consider an intracloud discharge initiated at the point of maximum vertical field above the negative charge region. Negative and positive leaders are assumed to develop simultaneously upward and downward from the initiation point along a single vertical channel. VHF mapping systems primarily observe the negative leader moving toward the upper positive charge region. The leader is assumed to be an approximate equipotential, with negative

Table 1. Charge Heights and Extents for the Cylindrical Disk Model of Figure 5 and Charge Amounts Required to Initiate Intracloud Discharges[a]

Charge Layer	Altitude, km AGL	Depth, km	Radius, km	Charge, C
Upper positive	7.0	2.0	2.5	31.5
Main negative	4.0	2.0	2.0	−45.0
Lower positive	1.5	2.0	2.0	4.5

[a]As inferred from the lightning mapping data. AGL, above ground level.

Electric Field and Potential Profiles

Predicted Speeds - No Preconditioning
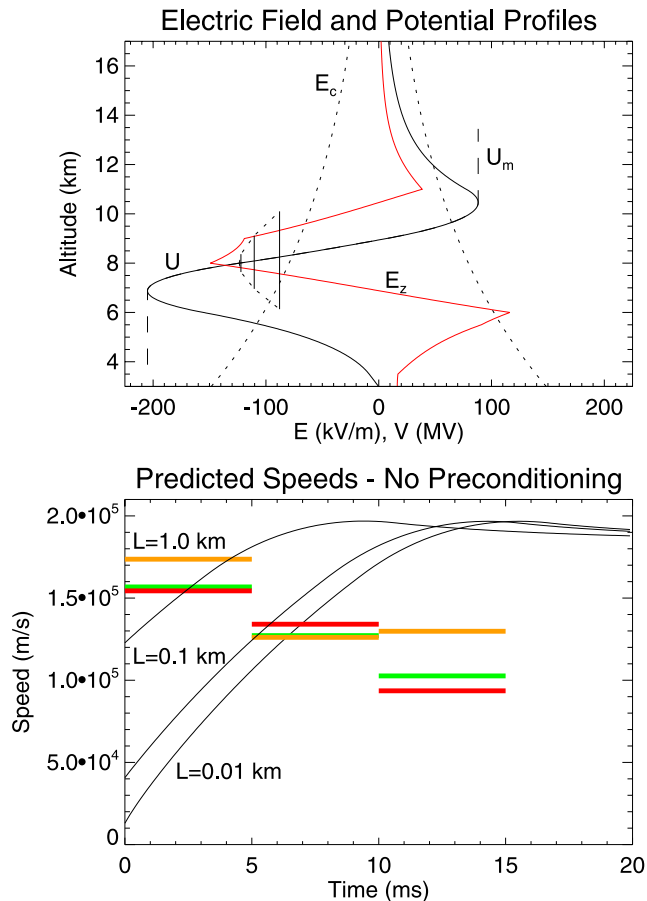
Figure 6. (top) Same as Figure 5, except showing the leader development for an assumed initial length $L = 10$ m. (bottom) Predicted leader speed assuming no preconditioning or dissipation for assumed initial lengths $L = 0.01$, 0.1, and 1.0 km and comparison with measured median speeds from Figure 4.

charge induced along its upper half and positive charge along its lower half. A large electric field is created at the leader tips that produces the electrical breakdown and sustains the leader propagation. As discussed by *Kasemir* [1960], the induced charge density along the channel is proportional to the difference ΔU between the channel potential and the ambient storm potential at the same altitude. To maintain overall charge neutrality in the presence of an asymmetric potential profile, the channel potential shifts as the leader extends its length [*Mazur and Ruhnke*, 1998; *Bazelyan and Raizer*, 2000]. The vertical lines in Figure 5 show this effect, wherein the leader potential was initially negative and increased with time, from -120 MV initially to -65 MV after 30 ms. As the leader extends it shorts out an increasingly large potential difference in the storm, increasing the potential gradient and electric field at its ends. As can be seen in Figure 5, the potential difference at the tips, ΔU_{tip}, quickly increases to more than 100 MV.

[23] *Bazelyan and Raizer* [2000] showed that the velocity of electron avalanche streamers immediately ahead of the advancing leader is proportional to the electric field at the

tip, and presented an empirical relation for the speed with which the leader advances. For positive leaders, the speed was given by

$$v_L = k \, \Delta U_{tip}^{1/2} \, , \qquad (1)$$

where, from laboratory measurements, $k = 15$ m s^{-1} V$^{-1/2}$. Although the streamer activity and propagation of negative leaders is more complex than for positive leaders, it is reasonable to assume that a similar power law relation exists between v_L and ΔU_{tip} for negative leaders, and that their speed increases with increasing potential difference. Therefore, and for lack of better information, we utilize (1) to estimate the breakdown speed on the expectation that its predictions will be a least qualitatively correct and to provide a framework for further assessment.

[24] To calculate the leader development corresponding to a given potential profile, we assume the leader is initiated at the local extremum in E_z and has an initial length L. The leader is grown in 1 ms steps according to (1); after each step the potential is adjusted to maintain zero net charge on the leader. The vertical lines in Figure 5 indicate the length and potential of the simulated leader every 5 ms over a 30 ms time interval. The initial length of the leader for the Figure 5 simulation was $L = 100$ m. The simulation assumes that once the leader tip reaches the potential extrema associated with the main negative and upper positive charge regions, it begins to propagate horizontally through the charge region at a fixed potential difference corresponding to the extremum values. Because the leader model is one-dimensional, we artificially and arbitrarily simulate the horizontal development by modifying the ambient potential profile to extend the extremum values 3 km beyond the extremum altitudes, as indicated by the dashed lines in Figure 5.

[25] Figure 6 shows the leader development for a shorter initial length ($L = 10$ m; Figure 6 (top)) and the calculated propagation speeds for three different initial lengths ($L = 10$ m, 100 m, and 1.0 km; Figure 6 (bottom)). The simulations are shown only for the initial 20 ms of breakdown. Also shown are the measured median speed values from Figure 4. The speeds from the simulations clearly do not agree with the measurements. The disagreement is twofold: First, the starting speed is significantly less than the measured speeds, particularly for short initial channel lengths. Second and more importantly, the predicted speed increases with time while the observations show the opposite, namely, deceleration from the initial value.

[26] If the constant of proportionality k for negative leaders were such as to bring the initial speed into agreement with the observations, both the speed increase and final speed value would be even more inconsistent with the observational results. The simulations agree with the observations in that the final speed has an approximate equilibrium value, but give a higher value than observed. In the model results, the equilibrium speed is associated with the potential difference reaching a maximum value, on the order of 100 MV at each end of the leader. Rather than corresponding to a maximum speed, however, the observational results show the final speed to be a minimum, suggesting that the initial speeds are enhanced relative to the final equilibrium values.

[27] We note at this point that the predicted speed increase is indeed observed in triggered lightning studies. As described by *Rakov and Uman* [2003, pp. 270–271], V. P. Idone (State University of New York at Albany) obtained photographs of the upward positive leader of a rocket-trailing wire that showed that the leader speed increased with height, from 1.2×10^5 m s^{-1} when first imaged to 6.5×10^5 m s^{-1} as the leader exited the field of view. Also, simulations of leaders using detailed breakdown models predict leader acceleration. Using the physical breakdown model of *Gallimberti et al.* [2002], *Lalande et al.* [2002] simulated the development of both the positive and negative leaders of a bidirectional altitude-triggered flash which showed acceleration of both leaders away from the 160-m-long triggering wire. A difference between the triggered lightning and intracloud results is that the electric fields close to the ground are well below the critical field value for energetic breakdown.

[28] A few intracloud discharges have been found whose leaders accelerated upward, but this was uncommon and tended to occur in discharges whose initial development was horizontal.

4. Effects of Preconditioning

[29] The observations of a greater initial speed and a smaller final speed can be explained if it is assumed that the leader channel is impulsively preconditioned in some manner, and that the preconditioning dies out either with time or distance to cause the leader to decelerate with time. The preconditioning would have to be sufficiently strong for its decay to overcome the tendency for the velocity to increase caused by the increasing potential difference.

[30] Such preconditioning would be provided by energetic electron avalanches. There is an increasing body of evidence, both theoretical and experimental, that electron avalanches occur in storms and can have important electrical effects [e.g., *Gurevich et al.*, 1992; *Gurevich and Zybin*, 2001; *Solomon et al.*, 2001; *Eack et al.*, 1996]. The studies have focused on the details of the runaway breakdown and resulting ionization, and the role this might play in initiating lightning discharges. However, electron avalanches would also affect other aspects of the lightning discharge. In particular, the avalanche process would be responsible for generating metastable molecules and ions that contribute to the fast propagation of the initial leader. As the metastable states dissipate, the leader speed would decrease.

[31] Physically, the preconditioning will dissipate with time due to the attachment of ions to water molecules creating cluster molecules, which then attach to cloud particles. The metastable states of oxygen and nitrogen have half lives ranging from hundreds of microseconds up to seconds [*Hartmann and Gallimberti*, 1975]. Outside the high field region energetic electrons will not avalanche, but will still produce ionization and metastable states. Therefore the farther the leader travels away from the high field region, the smaller the preconditioning effect becomes. In this way the preconditioning would decrease spatially.

[32] An attempt to model the above processes physically is beyond the scope of this study. Rather, we note that the effect of impulsive preconditioning would be to temporarily increase the constant of proportionality k in the empirical

relation (1) for the leader velocity, then to decrease k to its background or unconditioned value. We use this to determine an altered empirical relationship that would fit the observations. For simplicity we consider the temporal and spatial effects separately. For temporal decay, k is assumed to be given by

$$k = k_0 + k_1 e^{-t/\tau} , \qquad (2)$$

namely, to start out with a (spatially uniform) value $k = k_0 + k_1$ immediately following an energetic avalanche and to decrease exponentially to a nonpreconditioned value k_0, with a time constant τ. The spatial variation of the preconditioning effect, due either to a single energetic avalanche or to the steady state condition established by the background of energetic avalanche or ionization events, is assumed to be a function of the threshold factor E_z/E_c, according to

$$k = k_0 + k_2 (E_z/E_c)^x . \qquad (3)$$

Thus $k = k_0 + k_2$ when $E_z = E_c$ and $k = k_0$ for $E_z \ll E_c$. The model parameters are k_0, k_1, and τ for the temporal case and k_0, k_2 and the power law parameter x for the spatial case.

[33] Figure 7 shows the results of using the above approach to fit the observations. Figure 7 (top) shows the simulated leader development for the temporal decay case. The leader was initiated not at the point of the field extremum but just below the upper extent of the superthreshold field region, where upward developing electron avalanches would produce the strongest space charge concentrations. It was necessary to assume the higher initiation altitude in order for the spatial decay case to fit the observations; otherwise the leader would accelerate for a longer time than observed. For purposes of comparison, the same initiation altitude was also used for the temporal decay case. A side effect of the higher initiation altitude is that the leader potential is initially close to ground potential and shifts leftward instead of rightward as it develops.

[34] Figure 7 (bottom) shows the leader speeds calculated for the temporal and spatial decay cases. In both instances, the initial length of the leader was assumed to be 100 m. To best fit the observations, for the temporal decay case the time constant τ was 3 ms. For the spatial case, it was assumed that the preconditioning increases k as the square of the critical field ratio (E_z/E_c), namely, that the exponent $x = 2$ in expression (3). This choice for the power law dependence is not completely arbitrary, as it corresponds to the preconditioning being proportional to the (relative) energy density of the field.

[35] The parameter k_0 determines the final value of the leader speed. In both cases the best fit of the final speed corresponded to $k_0 = 8$; this is a factor of two less than the estimated value from (1) for positive leaders. The remaining parameters affect the initial speed and had best fit values of $k_1 = 40$ for the temporal decay case (solid line), and $k_2 = 9$ for the spatial decay case (dashed line). The measured median speed values are overlaid for comparison.

[36] The model-calculated leader speed increases within the first 2 ms of initiation but then begins to slow due to the temporal or spatial decreases in the preconditioning. Be-

Electric Field and Potential Profiles

Predicted Speeds - Preconditioned
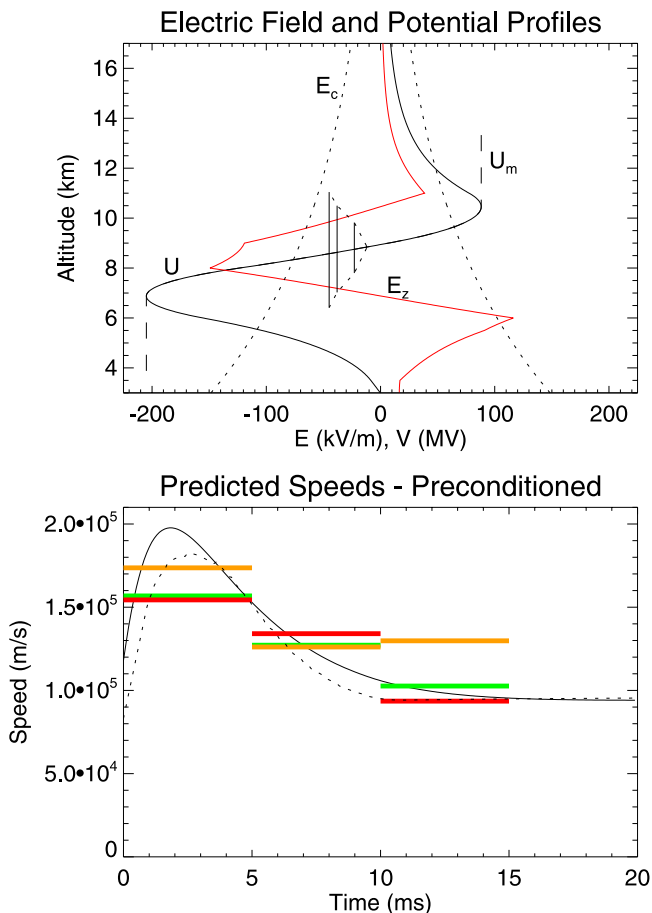
Figure 7. Same as Figure 6, except with the constant of proportionality k modified to simulate the effects of preconditioning and dissipation, either temporally (solid line) or spatially (dashed line). The leader was initiated at higher altitude in the supercritical field region and its assumed initial length was $L = 0.1$ km.

cause only a couple of radiation events are typically located during the initial few ms of an intracloud discharge, the mapping observations provide insufficient time resolution to determine if the brief initial acceleration is present. The fitted speed values are otherwise in general agreement with the observations.

[37] The above procedure fits three features of the velocity curves (the initial and final speeds and the decay rate) using three free parameters. Therefore the fact that we are able to roughly fit the data does not in itself imply the correctness of the preconditioning idea. Rather, it gives the values of the empirical parameters that preconditioning or other explanations would have to satisfy to explain the observations.

5. Discussion

[38] Several studies have shown that preconditioning increases the speed of laboratory leaders. Indeed, it is not at all surprising that this would happen. *Vidal et al.* [2002] found that long discharges in the laboratory could be guided by ionized channels produced by a very short laser pulse.

While following the ionized channel, the leader traveled an order of magnitude faster than it did outside the ionized channel. *Hartmann and Gallimberti* [1975] found that the velocity of short sparks increased when the sparks occurred repetitively and were separated by less than 200 μs in time. They determined that vibrationally excited metastable N_2 remained in the air between repetitions and was responsible for the increased speed since any remaining ionization had been removed by the field. *Lowke* [1992] proposed that metastable oxygen was responsible for low breakdown voltages seen in the laboratory when the voltage of the electrodes was raised slowly.

[39] Other possible explanations for the observed deceleration or for preconditioning have been considered and are now briefly discussed. The first explanation is that the leader slows due to an increase in the potential drop per unit channel length as the leader continues to develop. Because of the inherent instability of the breakdown processes, however, such an increase in resistive losses with time would tend to quickly shut off the breakdown. The fact that the discharge continues for some time and distance would indicate the opposite, namely, that the resistive drop decreases with time, particularly during the initial stages of the leader. The negative resistance properties of discharges lead to either highly conducting, very hot channels or to channels that quickly cool and stop being conductive.

[40] A second possible explanation of deceleration is that as the leader increases in length it develops multiple "tips" because of branching or small-scale bifurcations that have the effect of reducing the field strength at any one tip, hence causing the leader to slow. While the observations indicate that side branching occurs on the scale of tens of meters, they also show that the overall development of upward negative leaders is dominated by a single channel. The channel or branch that is "out ahead" of the others will have the bulk of the potential difference at its tip and will not be significantly slowed by the presence of other branches.

[41] Alternatively, the effective radius of a single, dominant tip could increase as the leader increases in length, thus causing ΔU_{tip} to drop across a larger distance and reducing the electric field in which the leader develops. One way this could happen is if the radius of the corona region increased as the potential difference increased. However, this would imply that the fastest speeds would occur when the potential difference is the smallest, contrary to physical reasoning (ΔU_{tip} would have a negative exponent in the empirical relation (1), and leaders would speed up as they die out due to loss of potential difference).

[42] Another way the leader could slow is that for normal polarity discharges in which negative breakdown propagates upward in the cloud, the tip size would tend to increase with altitude as a result of decreasing pressure. This effect is has not been accounted for. It can be tested by studying the speeds of inverted polarity intracloud discharges, whose negative leaders propagate downward rather than upward and occur at similar altitudes. Other things being equal, such an explanation would predict that downward negative leaders would accelerate rather than decelerate as they grow. Studies are currently underway to test this question, so far with inconclusive results.

[43] A final possible explanation of the observations is that the inferred preconditioning could be produced by the occurrence of undetected positive leaders prior to the onset of the negative leader. This follows the ideas of *Griffiths and Phelps* [1976] that nonconducting positive streamers would be more easily initiated than conducting negative leaders. Negative charge would tend to be concentrated in the source region of repeated positive streamers that could produce the observed negative breakdown. We have found one instance in which electric field change measurements detected charge transfer for a few milliseconds prior to the detection of negative breakdown by the LMA. The charge transfer would have preconditioned the channel and indeed was followed by a highly energetic RF burst at the beginning of an otherwise normal cloud flash (*Thomas et al.* [2001, Figure 2], who discussed it only in the context of the source powers of intracloud radiation). So far, however, this flash appears to be a special case. We are currently obtaining detailed observations of close lightning flashes at Langmuir Laboratory that should provide additional information on this question. Prior observations of many flashes have so far not shown such an effect [e.g., *Shao and Krehbiel*, 1996; *Maggio et al.*, 2005].

[44] In summary, the measured speed of initial leaders develops in a manner that is not in accord with the expected behavior. The observations imply the presence of some sort of preconditioning that could be caused by energetic breakdown processes.

References

Bazelyan, E. M., and Y. P. Raizer (2000), *Lightning Physics and Lightning Protection*, 325 pp., Inst. of Phys. Publ., Bristol, UK.

Coleman, L. M., T. C. Marshall, M. Stolzenburg, T. Hamlin, P. R. Krehbiel, W. Rison, and R. J. Thomas (2003), Effects of charge and electrostatic potential on lightning propagation, *J. Geophys. Res.*, *108*(D9), 4298, doi:10.1029/2002JD002718.

Eack, K. B., W. H. Beasley, W. D. Rust, T. C. Marshall, and M. Stolzenburg (1996), Initial results from simultaneous observation of X rays and electric fields in a thunderstorm, *J. Geophys. Res.*, *101*, 29,637–29,640.

Gallimberti, I., G. Bacchiega, A. Bondiou-Clergerie, and P. Lalande (2002), Fundamental processes in long air gap discharges, *C. R. Phys.*, *3*, 1335–1359.

Griffiths, R., and C. Phelps (1976), The effects of air pressure and water vapour content on the propagation of positive corona streamers, *Q. J. R. Meteorol. Soc.*, *102*, 419–426.

Gurevich, A. V., and K. P. Zybin (2001), Runaway breakdown and electric discharges in thunderstorms, *Phys. Uspekhi*, *44*(11), 1119–1140, doi:10.1070/PU2001v044n11ABEH000939.

Gurevich, A. V., G. M. Milikh, and R. Roussel-Dupre (1992), Runaway electron mechanism of air breakdown and preconditioning during a thunderstorm, *Phys. Lett. A*, *165*, 463–468.

Hartmann, G., and I. Gallimberti (1975), The influence of metastable molecules on the streamer progression, *J. Phys. D*, *8*, 670–680.

Kasemir, H. W. (1960), A contribution to the electrostatic theory of a lightning discharge, *J. Geophys. Res.*, *65*, 1873–1878.

Krehbiel, P. R., R. J. Thomas, W. Rison, T. Hamlin, J. Harlin, and M. Davis (2000), GPS-based mapping system reveals lightning inside storms, *Eos Trans. AGU*, *81*, 21–22, 25.

Lalande, P., A. Bondiou-Clergerie, G. Bacchiega, and I. Gallimberti (2002), Observations and modeling of lightning leaders, *C. R. Phys.*, *3*, 1375–1392.

Lang, T. J., et al. (2004), The Severe Thunderstorm Electrification and Precipitation Study, *Bull. Am. Meteorol. Soc.*, *85*(8), 1107–1125, doi:10.1175/BAMS-85-8-1107.

Liu, X. S., and P. R. Krehbiel (1985), The initial streamer of intracloud lightning flashes, *J. Geophys. Res.*, *90*, 6211–6218.

Lowke, J. J. (1992), Theory of electrical breakdown in air–the role of metastable oxygen in molecules, *J. Phys. D*, *25*, 202–210.

Maggio, C. R., L. M. Coleman, T. C. Marshall, M. Stolzenburg, M. A. Stanley, T. Hamlin, P. R. Krehbiel, W. Rison, and R. J. Thomas (2005), Lightning initiation locations as a remote sensing tool of large thunderstorm electric field vectors, *J. Atmos. Oceanic Technol.*, in press.

Marshall, T. C., M. McCarthy, and W. D. Rust (1995), Electric field magnitudes and lightning initiation in thunderstorms, *J. Geophys. Res.*, *100*, 7097–7103.

Mazur, V., and L. H. Ruhnke (1998), Model of electric charges in thunderstorms and associated lightning, *J. Geophys. Res.*, *103*, 23,299–23,308.

Proctor, D. E. (1981), VHF radio pictures of cloud flashes, *J. Geophys. Res.*, *86*, 4041–4071.

Rakov, V. A., and M. A. Uman (2003), *Lightning: Physics and Effects*, 850 pp., Cambridge Univ. Press, New York.

Rison, W., R. J. Thomas, P. R. Krehbiel, T. Hamlin, and J. Harlin (1999), A GPS-based three-dimensional lightning mapping system: Initial observations in central New Mexico, *Geophys. Res. Lett.*, *26*, 3573–3576.

Shao, X. M., and P. R. Krehbiel (1996), The spatial and temporal development of intracloud lightning, *J. Geophys. Res.*, *101*, 26,641–26,668.

Schonland, B. F. J. (1956), The lightning discharge, *Handb. Phys.*, *22*, 576–628.

Solomon, R., V. Schroeder, and M. B. Baker (2001), Lightning initiation—Conventional and runaway-breakdown hypotheses, *Q. J. R. Meteorol. Soc.*, *127*, 2683–2704.

Thomas, R. J., P. R. Krehbiel, W. Rison, T. Hamlin, J. Harlin, and D. Shown (2001), VHF source powers radiated by lightning discharges, *Geophys. Res. Lett.*, *28*, 143–146.

Thomas, R. J., P. R. Krehbiel, W. Rison, S. J. Hunyady, W. P. Winn, T. Hamlin, and J. Harlin (2004), Accuracy of the Lightning Mapping Array, *J. Geophys. Res.*, *109*, D14207, doi:10.1029/2004JD004549.

Vidal, F., et al. (2002), The control of lightning using lasers: Properties of streamers and leaders in the presence of laser-produced ionization, *C. R. Phys.*, *3*, 1361–1374.

————————

S. A. Behnke, Langmuir Laboratory, New Mexico Institute of Mining and Technology, Socorro, NM 87801, USA. (sbehnke@nmt.edu)

P. R. Krehbiel, Physics Department, New Mexico Institute of Mining and Technology, Socorro, NM 87801, USA. (krehbiel@ibis.nmt.edu)

W. Rison and R. J. Thomas, Electrical Engineering Department, New Mexico Institute of Mining and Technology, Socorro, NM 87801, USA. (rison@ee.nmt.edu; thomas@nmt.edu)